Measurements Of Spallation Target-Moderator-Reflector Neutronics At The Weapons Neutron Research Facility

G. J. Russell, M. M. Meier, J. S. Gilmore,
R. E. Prael, and H. Robinson

Los Alamos Scientific Laboratory
Los Alamos, New Mexico 87545, U.S.A.

A. D. Taylor

Rutherford and Appleton Laboratories
Chilton, Diocot, OXON OX11 OQX, U.K.

ABSTRACT

Basic neutronics data initiated by 800-MeV proton spallation reactions are important to spallation neutron source development, electronuclear fuel production, and computer code validation. We are measuring angle- and energy-dependent neutron production cross sections, neutron spectra and production from thick targets, thermal and epithermal neutron spectra and surface and beam fluxes from moderators, and fertile-to-fissile conversion yields inside thick targets. Other experiments are planned. The measurements are being done at the Weapons Neutron Research facility on a variety of targets and target-moderator-reflector configurations. The experiments are relevent to the above applications and provide data to validate computer codes.

INTRODUCTION

Several laboratories throughout the world are building and designing intense pulsed and steady-state thermal and epithermal spallation neutron sources.[1-5] There is also some interest in utilizing high-energy particle accelerators for converting fertile material to fissile material.[6] At the Los Alamos Scientific Laboratory (LASL), we have a self consistent experimental program (using 800-MeV protons) relevant to the above applications, and pertinent to validating computer codes used in these applications. The 800-MeV proton source is the Clinton P. Anderson Meson Physics Facility (LAMPF). We conduct the experiments at the Weapons Neutron Research facility (WNR)[1]--See Fig. 1.

Differential measurements provide data to test the fundamental processes and assumptions employed in the Monte Carlo computer codes used to calculate spallation reactions. Integral measurements inherently provide more complicated data because they include the effects of particle transport and secondary processes. We describe here our experimental program (see Table I for a summary) and show some preliminary results. Specific measurements underway or completed are:

- angular-dependent neutron production cross sections from 0.5-800 MeV for targets of Aℓ, Cu, In, Pb, and depleted U,
- neutron spectra (at 90°) from 0.5-400 MeV for thick Ta and W targets,
- neutron production from thick targets of W, Pb, Th, and depleted U,
- fertile-to-fissile conversion yields inside Th and depleted U targets, and
- thermal and epithermal neutron spectra, and surface and beam fluxes from moderators.

We will compare all experimental data with calculated predictions. The Monte Carlo computer codes used in our computations are the Oak Ridge National Laboratory (ORNL) code HETC[7] for particle transport $\gtrsim 20$ MeV, and the LASL code MCNP[8] for neutron transport $\lesssim 20$ MeV. Our present version of HETC does not include fission when predicting particle production from nucleon and pion collisions with a fissile nucleus. A version of HETC which accounts for the fission process in uranium will soon be released by ORNL.[9]

NEUTRON PRODUCTION AND CONVERSION MEASUREMENTS

The LASL Fertile-to-Fissile Conversion (FERFICON) program is a cooperative effort with the Canadians at the Chalk River Nuclear Laboratory. The LASL experiments provide an extension to 800 MeV of similar measurements (but more exhaustive in numbers) conducted using the TRIUMF cyclotron in Vancouver, B.C. The Canadian measurements were done at proton energies of 350 and 480 MeV. The LASL FERFICON program consists of two parts: a) the determination of neutron production from thick targets, and b) the measurement

of fertile-to-fissile conversion yields inside thick targets.

Neutron Production

To determine target neutron production, we place a target inside a 2-m-diam by 2-m-high water-bath (see Fig. 2) and measure, using an array of bare and cadmium-covered gold foils, the axial and radial neutron flux distributions in the water. We beta count the 0.0025-cm-thick foils (without chemical separation) to determine the $^{197}Au(n,\gamma)^{198}Au$ reactions, and use the cadmium ratio to correct the gold activation for resonance neutron capture. We integrate the measured flux distributions over the water-bath volume to obtain the total neutron captures in the water.

The number of protons striking the target are found by passing them through a three-foil aluminum packet located just upstream of the target. We count the central 0.025-cm-thick foil with a Ge-Li detector system and determine the number of $^{27}Al(p,3pn)^{24}Na$, $^{27}Al(p,x)^{22}Na$, and $^{27}Al(p,x)^{7}Be$ reactions. In general, the proton distributions are strongly peaked at the center and have "wings" which do not fall off as rapidly as a circular bivariate (Gaussian-type) distribution (see Ref. 10).

The targets used in the measurements (a combination of solid and clustered cylinders) are depicted in Fig. 3; details of the targets are given in Table II. All targets were stopping-length targets (long enough to range-out 800-MeV protons). The thorium and (larger) uranium targets were stopping targets since essentially no protons leaked from them.

In an applied sense, the most useful quantity is the neutron yield from the target per proton (and not the total neutron captures in the water-bath per proton). The water-bath affects target neutron production in several ways:

- There is an energy above which neutrons from the target are lost from the water-bath.
- Spallation reactions with oxygen nuclei by high-energy neutrons and protons escaping from the target produce a distributed neutron source throughout the water-bath.
- The water-bath reflects neutrons back into the target to be captured, that is, the target can act as a neutron sink.

- The water-bath reflects neutrons back into the target, and these neutrons may cause "secondary" (n,f) and (n,xn) source-type reactions, that is, the target can act as a "secondary" neutron source. These latter neutrons supplement the "primary" spallation neutrons and attendant "primary" (n,f) and (n,xn) source-type reactions which occur in the absence of the water-bath.

The first two items in the above list tend to compensate each other and are not too dependent on target material and size; the last two items can compensate each other, however, the net effect is complicated and depends on target material and size. Because of these complications, we will compare calculated neutron captures in the water-bath with measured values.

Calculated neutronics for the FERFICON bare-targets are shown in Table III. In the computations, we mocked-up the geometry of the clustered targets exactly. The low-energy, $\lesssim$20 MeV, neutron-enhancement (ratio of low-energy leakage neutrons to low-energy spallation neutrons) is ~3% for tungsten, lead, and thorium, and ~21% for uranium. Note the number of low-energy neutron captures and fissions in the thorium and uranium targets.

We compare calculated neutronics of clustered targets with "equivalent" solid targets in Table IV. The heterogeneity effects in the clustered targets are not too great, ranging from ~1.7% for the thorium target to ~4.4% for the uranium target.

We show comparisons between our preliminary data and BNL Cosmotron results[11,12] in Table V. For comparable targets (except for the difference in target length), there is good agreement between experimental results. Our computations of water-bath neutron captures are underway; we will compute water-bath neutron captures using versions of HETC with and without fission competition during the evaporation process. As part of an effort to benchmark his new code, R. G. Alsmiller has recently computed the neutron captures in the water-bath for our uranium targets.[9] Alsmiller's results (which incorporate fission when predicting particle production for nucleon and pion collisions with a uranium nucleus) are shown in Table V. There is good agreement between our preliminary data and Alsmiller's computations.

Conversion Measurements

We will measure the axial distribution of fertile-to-fissile conversion yield (^{232}Th to ^{233}U or ^{238}U to ^{239}Pu) inside the 19-

rod thorium and 37-rod depleted uranium targets, and integrate this distribution over the target volume to obtain the total conversion yield. We will also measure the total number of fissions occuring in a target. We will determine fertile-to-fissile conversion using a Ge-Li detection system to observe the ^{233}Pa activity in the thorium target and the ^{239}Np activity in the depleted uranium target. The measured spatial conversion yield, integrated conversion yield, and total number of fissions will be compared with calculated predictions.

NEUTRON SPECTRA AND PRODUCTION CROSS SECTIONS

We have measured, at 90° to the proton beam, the neutron spectra from 0.5-400 MeV for the tantalum and tungsten production targets used in the WNR high-current target area. We have also measured angle- and energy-dependent (0.5-800 MeV) neutron production cross sections for aluminum, copper, indium, lead, and depleted uranium targets. These latter measurements were made at 0°, 30°, 45°, and 112° to the proton beam. The production cross section measurements were part of the Ph.D. thesis of S. D. Howe; he is preparing the data for publication. Preliminary results of the tantalum and tungsten neutron spectra measurements are given in Refs. 10 and 13.

Qualitatively, our neutron spectra and neutron production cross section measurements show reasonable agreement with calculations for energies $\lesssim$ 20 MeV; however, the measurements are consistently higher than the calculations by factors of 2-4 for energies $\gtrsim$ 20 MeV. The relatively good agreement between measured and calculated results at the lower energies is consistent with data described in Ref. 14. The underprediction of the calculations above $\sim$ 20 MeV is consistent with other results obtained using 740-MeV protons[15], but disagree with 450-MeV proton data.[16,17] Since calculations are generally used to predict the neutron source incident on a shield, the underprediction of the neutron yields above $\sim$ 50 MeV is relevant to shield design problems for spallation neutron sources.

THERMAL AND EPITHERMAL NEUTRON SPECTRA FROM MODERATORS

The research program utilizing the WNR high-current target

area requires thermal ($E \lesssim 1$ eV), epithermal (1 eV $\lesssim E \lesssim$ 100 keV), and fast (100 keV $\lesssim E \lesssim$ 400 MeV) neutrons. The tantalum (2.54-cm diam by 15.24-cm long) production target is water cooled and inside an aluminum canister. The tungsten (4.45-cm diam by 24.13-cm long) production target is water cooled and inside a stainless steel canister. The first 5 cm of the tungsten target has a tapered reentrant hole (2.54-cm diam to 1.42-cm diam). We use the water-cooled tantalum target by itself for fast neutron production, and polyethylene moderators around the tantalum target (in a hybrid slab geometry--see Fig. 4a) for epithermal neutron production. Optimum thermal neutron production is a more complicated issue.

For spallation neutron sources, a reflected moderator can increase thermal neutron beam fluxes by a factor of 2-4 over a bare moderator. There are also significant differences (factor of 2) in thermal neutron intensities between center-looking (where the field-of-view looks at the target) and offset geometry (where the target is not viewed directly). However, in center-looking geometry there can be substantial contamination of thermal neutron beams with higher-energy neutrons and charged particles; these beam-contaminants may cause unwanted background problems.

Total neutron production from a target is not necessarily a definitive indicator of resultant thermal neutron beam fluxes. A particular target-moderator-reflector configuration needs to be assessed as an integral unit relative to thermal neutron generation. We studied theoretically the neutronics of several unreflected target-moderator geometries (see Fig. 4b and Ref. 18), and will measure absolute thermal neutron production from a variety of target-moderator-reflector configurations. In addition to the unreflected hybrid slab-moderator (which was the initial target-moderator geometry installed in the WNR high-current target area[19]--see Figs. 4a and 5a), we are studying several reflected target-moderator configurations. The reflected geometries are depicted in Figs. 5b, 6a, and 6b.

The experiments are conducted in the WNR low-current target area. We measure, using bare and cadmium-covered gold foils, the absolute value of the thermal and epithermal neutron beam fluxes, and the spatial distribution of the thermal and epithermal neutron

fluxes at the surface of a moderator. We also use BF_3 and fission detectors to measure thermal and epithermal neutron spectra. Proton monitoring has been mainly done using aluminum foils. We are presently evaluating on-line methods of proton detection such as toroids and secondary emission monitors, and are calibrating these devices on an absolute basis. We present here some preliminary results from our target-moderator-reflector development program.

Reflected Wing-Moderator

The initial reflected wing-moderator studied is shown in Figs. 6a and 7. We placed the target (a cylinder of depleted uranium, 10.0-cm diam by 40.7-cm long) in a stainless steel canister. There was an air gap (~ 1 cm) between the uranium and the outside of the canister. The low-density polyethylene premoderator was 5.0-cm thick, poisoned with 0.076-cm of cadmium and backed with a 1.27-cm-thick high-density polyethylene moderator. The beryllium reflector was essentially a cube with ~ 66-cm-long sides, and was decoupled from the polyethylene by 0.076-cm of cadmium. The wing-moderator was located 2 cm from the front surface of the target.

We define the 2200 m/s neutron flux, φ_o, to be the activations in a gold foil by neutrons with energies < 0.5 eV divided by the 2200 m/s gold cross section. The Maxwellian thermal neutron flux, φ_m, is related to φ_o by Eq. (1)--Ref. 20,

$$\varphi_m = \frac{1}{g(T)} \frac{2}{\sqrt{\pi}} \left(\frac{T}{T_o}\right)^{\frac{1}{2}} \varphi_o , \qquad (1)$$

where g(T) is the non-1/v factor, T is the absolute temperature of the neutrons, and T_o = 293.6 ^oK. Some preliminary spatial distributions of φ_o at the moderator surface are shown in Figs. 8a and 8b. Note the rapid falloff of the neutron flux with distance from the target; the neutron flux in the direction of the target axis is fairly symmetric. An average $\bar{\varphi}_o$ (over ~ 78 cm^2 of moderator surface) is $\bar{\varphi}_o \approx 1.8 \times 10^{-3}$ n/cm^2. p.

We plan to make further measurements using the reflected wing

geometry, however, the number of moderators will be increased to four. We will study the effect, on thermal neutron beam fluxes, of varying the target material and diameter, and of altering the target-moderator-reflector decoupling. We will measure absolute thermal neutron beam fluxes, spectra, and pulse widths for both the "upstream" and "downstream" moderators.

Reflected 'T'-Shape Moderator

The layout of the flight paths in the WNR high-current target-area is shown in Fig. 9. The flight paths are clustered in groups of three, and there is a cluster in each quadrant. The reflected 'T'-shape moderator shown in Figs. 10a and 11 makes reasonable use of the existing flight path arrangement, and provides for a number of concurrent thermal neutron beam experiments. For similar moderators, the thermal neutron beam fluxes from the various "legs" of the 'T'-shape moderator are essentially the same. This is in contrast to the reflected-wing geometry with multiple moderators where factors of two in thermal neutron beam fluxes between the "upstream" and "downstream" moderators can be expected.[21] With the 'T'-shape configuration, the flight paths view the moderators in offset geometry. The premoderator-moderator concept allows each moderator to be optimized (as illustrated in Fig. 10b) for a particular class of instruments using thermal neutron beams.

We have recently installed a prototype reflected 'T'-shape moderator in the WNR high-current target area. The reflector is a composite of polyethylene and beryllium; cadmium is used as the neutron decoupler. We presently have a development program to optimize the reflected 'T'-shape moderator and reflector. We will replace the prototype 'T'-shape configuration with an "optimized" version when our studies are complete.

We have made some preliminary neutronic measurements with a reflected 'T'-shape moderator. The configuration studied is illustrated in Figs. 10a and 11. In the experiments, we are using three targets (lead, tungsten, and depleted uranium). Each target is 4.45-cm diam by 24.13-cm long. The first 5 cm of each target has a tapered reentrant hole (2.54-cm diam to 1.42-cm diam). With the exception of the reentrant hole, the targets are solid. For handling convenience, each target is encapsulated in a stainless steel tube. In addition, the depleted uranium target has a

0.076-cm-thick cadmium layer between the target and stainless steel canister. The purpose of the cadmium is to offer some neutronic decoupling between the moderator-reflector and the target. Calculated neutronics of the bare-targets are shown in Table VI. Note for the uranium target that the low-energy ($\lesssim 20$ MeV) neutron enhancement via (n,f)- and (n,xn)-type reactions is $\sim 14\%$.

The low-density polyethylene premoderator was poisoned with 0.076-cm of cadmium and backed with a 1.27-cm-thick high-density polyethylene moderator. The beryllium reflector was roughly cubic with ~ 61-cm-long sides, and was decoupled from the polyethylene by 0.076-cm of cadmium.

We constructed an experimental setup to specifically measure thermal and epithermal neutron beam fluxes and spectra; we will be adding the capability of measuring neutron pulse widths in the near future. We have made the following changes in experiment parameters and looked at the effects on thermal neutron beam fluxes and spectra:

- varied the target material (lead, tungsten, and depleted uranium),
- changed the premoderator material (polyethylene, water, and titanium hydride),
- altered the poison (cadmium and gadolinium) between the premoderator and moderator,
- varied the moderator thickness,
- used reentrant-type moderators,
- removed the moderator and its decoupler, and looked at the premoderator itself,
- changed the shadow-bar material (polyethylene, beryllium, copper, and tungsten), and
- varied the size of the reflector.

The data are being analyzed. Absolute thermal neutron beam fluxes and spectra will be reported. Results comparing the effects of using different types of targets are shown in Table VII. The calculated neutronic enhancement for depleted uranium (relative to lead and tungsten) is somewhat lower than that measured using thermal neutron beam fluxes. This may indicate a deficiency in the code package used (our present version of HETC does not

account for uranium fission), or illustrate that energy neutronic decoupling is needed between the uranium target and the moderator-reflector.

Results of moderator variation are presented in Table VIII. We found gadolinium (0.0025-cm-thick) to be superior to cadmium (0.076-cm thick) as a poison material at a given depth. A marked increase in moderation is found as the depth of poisoning is increased. However, thermal neutron beam fluxes alone are not sufficient to assess target-moderator-reflector performance; thermal neutron pulse widths are also important. The thermal and epithermal neutronic performance is degraded by increasing the premoderator thickness. (An optimization of material and thickness for the 'T'-shape premoderator and reflector will be the subject of a future study.) For the 'T'-geometry, mini-reentrant moderators produced no enhancement of the thermal neutron flux, although a significant lowering of the neutron temperature was observed. Our results for reentrant-type moderators disagree with measurements made by others.[22] However, the criteria used in all three measurements (geometric coupling, conservation of moderator thickness or mass, etc.) differed. In particular, our results may be very dependent upon which "leg" of the 'T'-shape moderator is viewed. We will continue to study thermal neutron beam fluxes, spectra, and pulse widths from reentrant-type moderators.

A sample of the raw time-of-flight data obtained with our BF_3 detector (nominally 13% efficient for neutrons of energy 0.025 eV) is shown in Fig. 12. The data are shown as neutron spectra, $\varphi(E)$, in Fig. 13. The Maxwellian temperature is ~ 380 ^{o}K. The data in Figs. 12 and 13 are for the tungsten target, a low-density polyethylene moderator, and a 1.27-cm-thick high-density polyethylene moderator decoupled by a 0.076-cm layer of cadmium, the beryllium reflector was a cube with sides ~ 61-cm long.

FUTURE PLANS

We will continue our measurements of neutron production and neutron production cross sections using other target materials and angles. Fertile-to-fissile conversion yields will be measured

this fiscal year. We will measure thermal neutron beam fluxes, spectra, and pulse widths in a continuing study of target-moderator-reflector configurations, these studies will include the effects of changing decoupler materials between the target-moderator-reflector. We will measure thin-target neutron production using bath techniques, and plan to measure neutron spectra from thick bare-targets. We will measure cold moderator neutron beam fluxes, spectra, and pulse widths. We could also measure neutron production and fertile-to-fissile conversion yields inside massive (~ 2000 kg) thorium and uranium targets. Energy deposition in spallation targets and cold moderators is another area where we could make relevent measurements.

ACKNOWLEDGEMENTS

This work was performed under the auspices of the U.S. Department of Energy. We would like to acknowledge the support and encouragement of R. Woods, and useful discussions with J. L. Yarnell, and J. S. Fraser. We appreciate the help of J. R. Baldonado and K. J. Hughes in setting up the experiments, and of P. R. Martinez for typing assistance. We acknowledge the cooperation of E. R. Whitaker, the WNR operations crew of R. D. Ryder (head), H. M. Howard, R. A. Johnson, and M. R. Lopez, and the help of the CNC-11 counting room personnel.

REFERENCES

1. G. J. Russell, P. W. Lisowski, and N. S. P. King, "The WNR Facility--A Pulsed Spallation Neutron Source at the Los Alamos Scientific Laboratory," Intl. Conf. on Neutron Physics and Nucl. Data for Reactors and Other Appl. Purposes, Harwell, England (1978).

2. L. C. W. Hobbis, G. H. Rees, and G. C. Stirling, eds., "A Pulsed Neutron Facility for Condensed Matter Research," Rutherford Laboratory report RL-77-064/C (1977).

3. J. M. Carpenter, D. L. Price, and N. J. Swanson, eds., "IPNS--A National Facility for Condensed Matter Research," Argonne National Laboratory report ANL-78-88 (1978).

4. Y. Ishikawa, ed., "KENS Report I," KEK Internal report 80-1 I/B (May 1980).

5. G. S. Bauer, ed., "Targets for Neutron Beam Spallation Sources," Jül-Conf-34, ISSN 0344-5798, Jülich (1980).

6. H. J. C. Kouts and M. Steinberg, eds., "Proc. of an Information Meeting on Accelerator-Breeding," ERDA Conf-770107, Brookhaven National Laboratory (1977).

7. K. C. Chandler and T. W. Armstrong, "Operating Instructions for the High Energy Nucleon Meson Transport Code HETC," Oak Ridge National Laboratory report ORNL-4744 (1972).

8. W. L. Thompson, ed., "MCNP - A General Monte Carlo Code for Neutron and Photon Transport," Los Alamos Scientific Laboratory report LA-7396-M (1979).

9. R. G. Alsmiller, Jr., et al., "Thermal Neutron Flux Generation by Medium-Energy (< 1.5 GeV) Protons in Thick Uranium Targets," Oak Ridge National Laboratory report ORNL/TM-7527 (1980).

10. G. J. Russell, et al., "Spallation Target-Moderator-Reflector Studies at the Weapons Neutron Research Facility," Proc. of Symposium on Neutron Cross-Sections from 10 to 50 MeV, BNL-NCS-51245, Vol. I, 169-191, Brookhaven National Laboratory (1980).

11. J. S. Fraser, et al., "Neutron Production by Thick Targets Bombarded by High-Energy Protons," Physics in Canada, Vol. 21 No. 2, 17-18 (1965).

12. P. M. Garvery, "Neutron Production by Spallation in Heavy Metal Targets," Proc. of Meeting on Targets for Neutron Beam Spallation Sources, Jül-Conf-34, ISSN 0344-5798, Jülich (1980).

13. S. D. Howe, et al., "Neutron Spectrum at 90° from 800-MeV (p,n) Reactions on a Ta Target," Proc. Conf. on Nuclear Cross Sections for Technology, Knoxville (1979) - to be published.

14. L. R. Veeser, et al., "Neutrons Produced by 740-MeV Protons on Uranium," Nucl. Inst. Meth., 17, 509-512 (1974).

15. R. Madey and F. M. Waterman, "High-Energy Neutrons Produced by 740-MeV Protons on Uranium," Phys. Rev. C, Vol. 8 No. 6, 2412-2418 (1973).

16. J. W. Wachter, W. A. Gibson, and W. R. Burrus, "Neutron and Proton Spectra From Targets Bombarded by 450-MeV protons," Phys. Rev. C, Vol. 6 No. 5, 1496-1508 (1972).

17. R. G. Alsmiller, Jr., "Calculation of the Neutron and Proton Spectra from Thick Targets Bombarded by 450-MeV Protons and Comparison with Experiment," Nucl. Sci. Engr., 36, 291-294 (1969).

18. G. J. Russell, P. A. Seeger, and R. G. Fluharty, "Parametric Studies of Target/Moderator Configurations for the Weapons Neutron Research (WNR) Facility," Los Alamos Scientific Laboratory report LA-6020 (March 1977).

19. G. J. Russell, "Initial Target/Moderator Configuration for the Weapons Neutron Research Facility," Trans. Am. Nucl. Soc., 27, 861-862 (1977).

20. K. H. Beckurts and K. Wirtz, Neutron Physics, Springler-Verglag, New York, Inc. (1964).

21. A. D. Taylor, "Neutron Transport from Targets to Moderators," Proc. of Meeting on Targets for Neutron Beam Spallation Sources, Jul-Conf-34, ISSN 0344-5798, Julich (1980).

22. G. S. Bauer and J. M. Carpenter, private communication at ICANS IV Conference (Oct. 1980).

TABLE I
PROGRAM FOR MEASURING SPALLATION TARGET-MODERATOR-REFLECTOR NEUTRONICS AT THE WEAPONS NEUTRON RESEARCH FACILITY

GENERAL GOALS

- Obtain basic data relevant to spallation neutron source development, accelerator breeder technology, and computer code validation
- 'Optimize' a target-moderator-reflector configuration for materials science research at the present WNR and any upgraded WNR
- Characterize WNR targets and moderators for nuclear physics applications

SPECIFIC OBJECTIVES

- Measure the effects of different targets, moderators, reflectors, and decouplers on thermal and epithermal neutron beam fluxes and thermal neutron pulse widths
- Ascertain the 'practical' gain of a uranium spallation target (versus lead, tantalum, tungsten, etc.) by measuring thermal neutron beam fluxes and pulse widths
- Measure the high-energy neutron and particle contamination in thermal neutron beams for offset and center-looking geometry
- Study neutron yields and pulse widths from cold moderators
- Measure neutron production and spectra from thin and thick targets
- Measure the fertile-to-fissile conversion yields inside thick targets of thorium and depleted uranium
- Measure energy deposition in spallation targets and cold moderators
- Compare all measurements with calculated predictions

TABLE II
PHYSICAL CHARACTERISTICS OF FERFICON TARGETS

TARGET MATERIAL	DENSITY (g/cm^3)	DIAMETER (cm)	LENGTH (cm)	^{235}U ENRICHMENT (wt%)
W[a]	18.26	4.45	24.13	----
Pb	11.31	9.85	40.65	----
U	18.4	10.01	40.65	0.198
Th	11.38	18.28[b]	40.65	----
U	19.04	20.09[c]	40.65	0.251

[a]The first 5 cm of the target had a tapered reentrant hole (2.54-cm diam. to 1.42-cm diam.)

[b]Effective diameter ($D = d\sqrt{n}$) for a 19 rod array with an individual rod diameter of 4.1928 cm.

[c]Effective diameter ($D = d\sqrt{n}$) for a 37 rod array with an individual rod diameter of 3.3035 cm.

TABLE IV
CALCULATED NEUTRONICS OF CLUSTERED AND SOLID BARE-TARGETS

	Th		U	
	Solid Target[a] 18.28-cm diam (n/p)	Clustered Target 19-Rod Array (n/p)	Solid Target[a] 20.09-cm diam (n/p)	Clustered Target 37-Rod Array (n/p)
LOW-ENERGY (< 20 MeV) SPALLATION NEUTRON PRODUCTION[b]	21.39±0.27	20.98±0.27	25.06±0.33	24.20±0.33
NEUTRON LEAKAGE (< 20 MeV)[c]	22.05±0.26	21.74±0.26	30.42±0.38	29.55±0.37
NEUTRON LEAKAGE (> 20 MeV)	0.97±0.02	1.05±0.02	0.71±0.02	0.79±0.02
TOTAL NEUTRON LEAKAGE	23.02±0.26	22.79±0.26	31.13±0.38	30.34±0.37
NEUTRON CAPTURE (< 20 MeV)[d]	1.51±0.02	1.32±0.02	4.44±0.06	3.72±0.06
TOTAL NEUTRON PRODUCTION	24.53±0.26	24.11±0.26	35.57±0.39	34.06±0.38
NEUTRON INDUCED FISSIONS [< 20 MeV] (fiss/p)	0.60±0.01	0.57±0.01	4.43±0.07	3.72±0.06

[a]Solid targets had an effective diameter $D = d\sqrt{n}$ where d is the diameter of an individual rod in a clustered target, and n is the number of clustered rods.

[b]Evaporation neutrons produced inside the target; fission competition with evaporation was not included in HETC.

[c]Includes net effects of (n,f)- and (n,xn)-type reactions occuring during the transport of low-energy spallation neutrons.

[d]Neutron capture occuring in a target during the transport of low-energy spallation neutrons.

TABLE III
CALCULATED NEUTRONICS FOR FERFICON BARE-TARGETS

	Solid Targets[a]			Clustered Targets[a]	
	W 4.45-cm diam (n/p)	Pb 9.85-cm diam (n/p)	U 10.01-cm diam (n/p)	Th 19-Rod Array[b] (n/p)	U 37-Rod Array[c] (n/p)
LOW-ENERGY (< 20 MeV) SPALLATION NEUTRON PRODUCTION[d]	13.15±0.16	16.12±0.20	21.37±0.27	20.98±0.27	24.20±0.33
NEUTRON LEAKAGE (< 20 MeV)[e]	13.47±0.17	16.55±0.20	25.84±0.32	21.74±0.26	29.55±0.37
NEUTRON LEAKAGE (> 20 MeV)	1.18±0.02	1.17±0.02	1.05±0.02	1.05±0.02	0.79±0.02
TOTAL NEUTRON LEAKAGE	14.65±0.17	17.72±0.20	26.89±0.32	22.79±0.26	30.34±0.37
NEUTRON CAPTURE (< 20 MeV)[f]	0.155±0.002	0.009±0.0002	1.05±0.02	1.32±0.02	3.72±0.06
TOTAL NEUTRON PRODUCTION	14.81±0.17	17.73±0.20	27.94±0.32	24.11±0.26	34.06±0.38
NEUTRON INDUCED FISSIONS [< 20 MeV] (fiss/p)	-------	-------	2.34±0.04	0.57±0.01	3.72±0.06

[a]Proton energy is 800 MeV; the W target was 24.13-cm long, and the first 5 cm had a tapered reentrant hole (2.54-cm diam to 1.42-cm diam); all other targets were 40.65-cm long.

[b]Individual rod diameter was 4.1928 cm.

[c]Individual rod diameter was 3.3035 cm.

[d]Evaporation neutrons produced inside the target; fission competition with evaporation was not included in HETC.

[e]Includes net effects of (n,f)- and (n,xn)-type reactions occuring during transport of low-energy spallation neutrons.

[f]Neutron capture occuring in a target during transport of the low-energy spallation neutrons.

TABLE V
PRELIMINARY LASL FERFICON RESULTS COMPARED TO BNL COSMOTRON DATA

TARGET MATERIAL	LASL FERFICON			BNL COSMOTRON[a]		
	LASL TARGET SIZE DIAMETER x LENGTH (cm x cm)	CALCULATED H_2O NEUTRON CAPTURES PER PROTON	MEASURED H_2O NEUTRON CAPTURES PER PROTON	BNL COSMOTRON TARGET SIZE DIAMETER x LENGTH (cm x cm)	CALCULATED H_2O NEUTRON CAPTURES PER PROTON[b]	MEASURED H_2O NEUTRON CAPTURES PER PROTON
W	4.45 x 24.13[c]		10.2	----	----	----
Pb	9.85 x 40.65		13.0	10.2 x 61.0	16.4	13.4
U	10.01 x 40.65	27.2±1.2[f]	25.3	10.2 x 61.0	23.3	26.3
Th	18.28 x 40.65[d]		17.1	----	----	----
U	20.09[e] x 40.65	28.6±0.8[f]	28.8	----	----	----

[a]Interpolated at 800 MeV (Ref. 10)

[b]Ref. 11

[c]The first 5 cm of the target had a tapered reentrant hole (2.54-cm diam to 1.42-cm diam)

[d]Effective diameter (D = d$\sqrt{7}$i) for a 19-rod array with an individual rod diameter of 4.1928 cm.

[e]Effective diameter (D = d$\sqrt{7}$i) for a 37-rod array with an individual rod diameter of 3.3035 cm.

[f]Ref. 9

TABLE VI
CALCULATED NEUTRONICS FOR BARE (REENTRANT) TARGETS[a]

	Pb (n/p)	W (n/p)	U (n/p)
LOW-ENERGY (< 20 MeV) SPALLATION NEUTRON PRODUCTION[b]	11.34±0.16	13.25±0.16	16.88±0.23
NEUTRON LEAKAGE (< 20 MeV)[c]	11.52±0.16	13.59±0.16	19.16±0.27
NEUTRON LEAKAGE (> 20 MeV)	1.10±0.02	1.18±0.02	1.21±0.02
TOTAL NEUTRON LEAKAGE	12.62±0.16	14.77±0.16	20.37±0.27
NEUTRON CAPTURE (< 20 MeV)[d]	0.002±0.00003	0.16±0.002	0.22±0.003
TOTAL NEUTRON PRODUCTION	12.62±0.16	14.93±0.16	20.59±0.27
NEUTRON INDUCED FISSIONS [< 20 MeV] (fiss/p)	----------	----------	1.01±0.02

[a]Targets were 24.13-cm long; the first 5 cm had a tapered reentrant hole (2.54-cm diam to 1.42-cm diam); uniform proton beam spot (1.5-cm diam).

[b]Evaporation neutrons produced inside the target; fission competition with evaporation was not included in HETC.

[c]Includes net effects of (n,f)- and (n,xn) -type reactions occuring during transport of low-energy spallation neutrons.

[d]Neutron capture occuring in a target during transport of the low-energy spallation neutrons.

TABLE VII
RELATIVE PERFORMANCE OF SPALLATION TARGETS

Target Material[a]	Ratio of Calculated Spallation Neutron Production[b]	Ratio of Calculated Low-Energy Neutron Leakage[c]	Ratio of Measured Thermal Neutron Beam Flux[d]
Pb	1.00	1.00	1.00
W	1.17	1.18	1.25
U	1.49	1.66	2.13

[a]Targets were 24.13-cm long; the first 5 cm had a tapered reentrant hole (2.54-cm diam to 1.42-cm diam); 1.5-cm-diam uniform proton beam spot assumed; 800-MeV incident protons.

[b]Low-energy (< 20 MeV) evaporation neutrons produced inside a bare target; fission competition with evaporation was not included in HETC.

[c]Leakage neutrons (< 20 MeV); includes net effects of (n,f)- and (n,xn)-type reactions occuring during transport of low-energy spallation neutrons.

[d]'T'-shape polyethylene moderator reflected by beryllium; the uranium target was decoupled from the polyethylene moderator by 0.076 cm of cadmium.

TABLE VIII
SUMMARY OF MODERATOR SPECTRAL MEASUREMENTS

ALL DATA TAKEN WITH A TUNGSTEN TARGET AND A 'T' SHAPED PREMODERATOR SURROUNDED BY A 46 cm CUBE BERYLLIUM REFLECTOR AND DECOUPLED BY 0.076 cm OF CADMIUM.

A. 1.27 cm POLYETHYLENE MODERATOR: VARIATION OF POISON AND PREMODERATOR

MODERATOR	T[a] (meV)	J_{th}[a]	$E\phi(E)|_{1eV}$[b]	$J_{th}/E\phi(E)|_{1eV}$	SUB - Cd[c]
1.27 cm poisoned by Gd[d]	35	61	23	2.7	1.00
1.27 cm poisoned by Cd[e]	33	37	22	1.7	0.64
1.27 cm poisoned by Gd with additional 1.27 cm of premoderator	34	52	20	2.6	0.83

B. POLYETHYLENE MODERATORS 2.54 cm THICK AND POISONED BY Gd[d]: MINI-REENTRANT HOLE STUDY

MODERATOR	T (meV)	J_{th}	$E\phi(E)|_{1eV}$	$J_{th}/E\phi(E)|_{1eV}$	SUB - Cd
No holes	34	92	20	4.6	1.16
0.64 cm deep circular holes[f]	32	91	20	4.6	1.21
1.27 cm deep circular holes	30	81	21	3.9	1.20
1.91 cm deep circular holes	30	62	23	2.7	1.09
1.91 cm deep grooves[g]	30	76	21	3.6	1.16

C.. MODERATORS POISONED BY Gd[d] VARIATION OF POISON DEPTH

MODERATOR	T (meV)	J_{th}	$E\phi(E)|_{1eV}$	$J_{th}/E\phi(E)|_{1eV}$	SUB - Cd
0.64 cm polyethylene	42	45	25	1.8	0.89
1.27 cm polyethylene	35	61	23	2.7	1.00
1.91 cm polyethylene	34	84	21	4.0	1.13
2.54 cm polyethylene	34	92	20	4.6	1.16
Premoderator only No poison	33	237	26	9.1	2.59

[a]The apparent maxwellian temperature, T, and the maxwellian intensity, J_{th}, are determined by a fitting

$$\phi = J_{th} \frac{E}{T^2} \text{ EXP } [-E/T]$$

in the range 0 – 50 meV. See figure 20. Units are arbitrarily normalized to incident protons.

[b]The 1eV lethergy is obtained by fitting in the range 1 – 10 eV. See figure 19. Units are arbitrarily normalized to incident protons.

[c]Relative sub-cadmium fluxes normalized to the 1.27 cm, Gd poisoned moderator.

[d]0.0025 cm gadolinium foil

[e]0.076 cm cadmium sheet

[f]81 0.79 cm diameter, straight sided holes. 40% of area removed.

[g]Tapered grooves, 0.4 cm at base and top

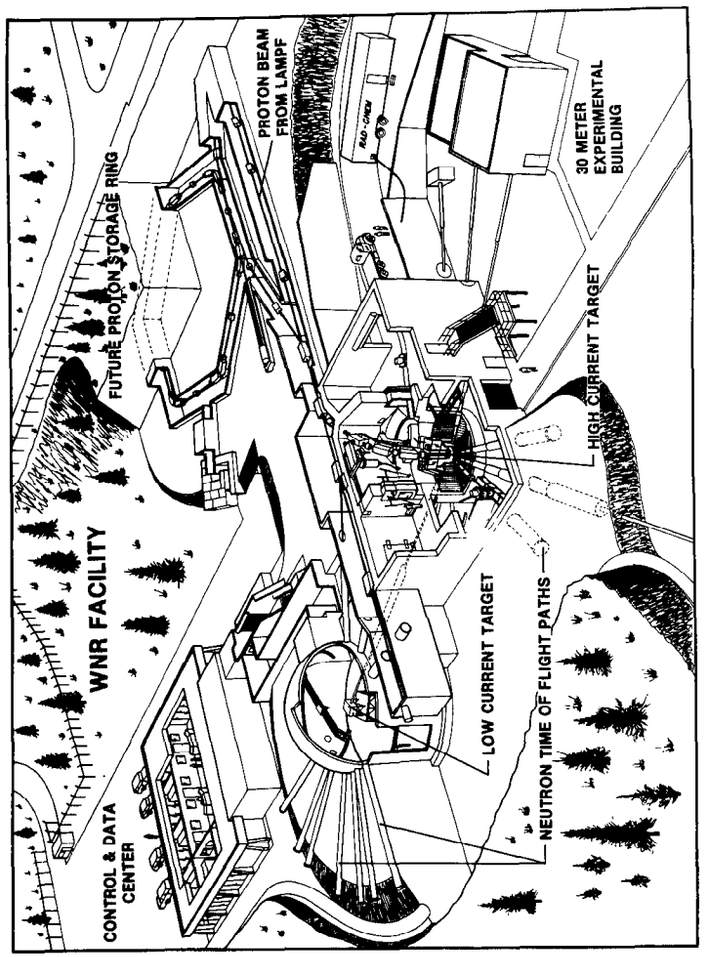

Fig. 1 General layout of the WNR showing the two target areas. The high-current target is located in a vertical proton beam and is viewed by 11 horizontal flight paths. The low-current target is located in a horizontal proton beam and viewed by 12 horizontal flight paths and one vertical flight path.

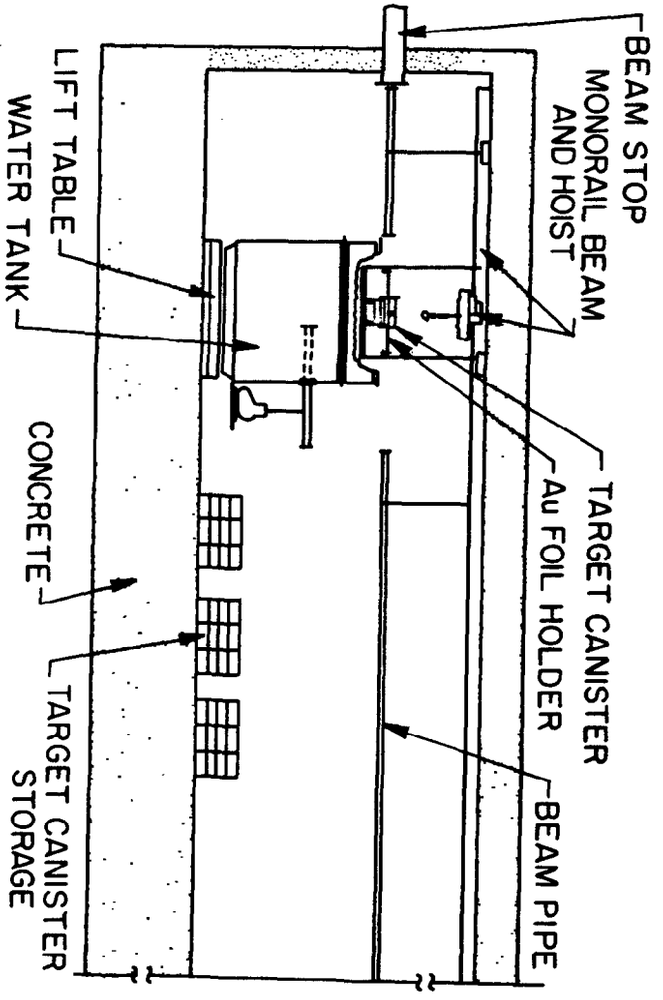

Fig. 2 Section through the WNR beam channel showing the location of the FERFICON experiment.

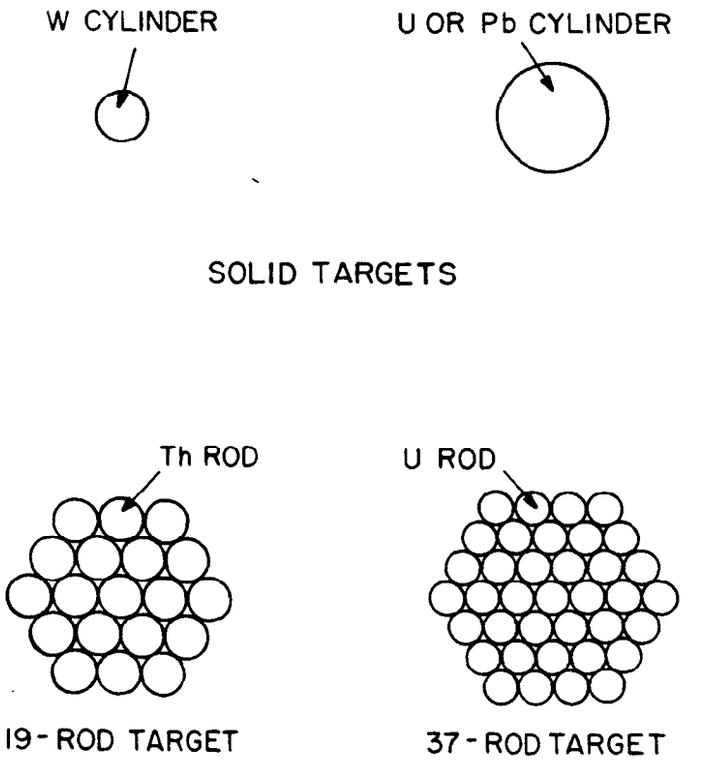

Fig. 3 Targets used in the LASL FERFICON experiments (relative sizes are as indicated).

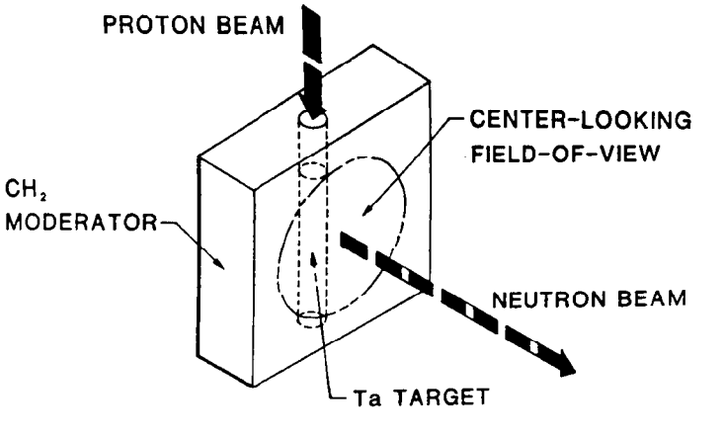

Fig. 4a Unreflected hybrid slab-moderator used at the WNR to produce neutrons with energies 1 eV $\lesssim E \lesssim$ 100 keV.

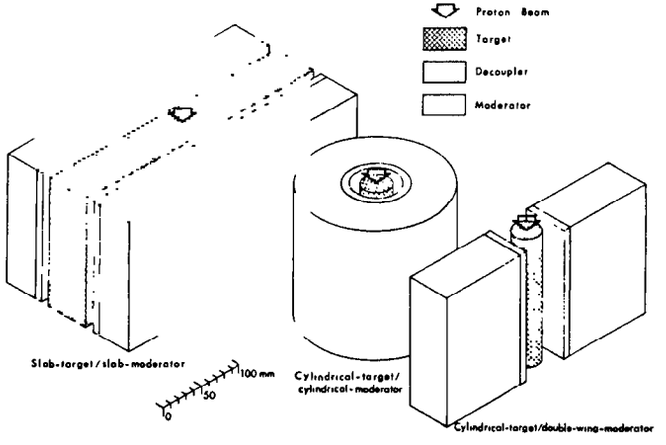

Fig. 4b Several unreflected target-moderator configurations studied theoretically.

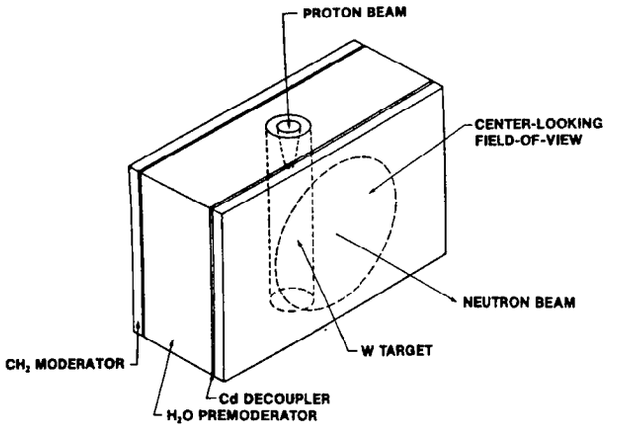

Fig. 5a Unreflected hybrid slab-moderator initially used at the WNR for thermal neutron production.

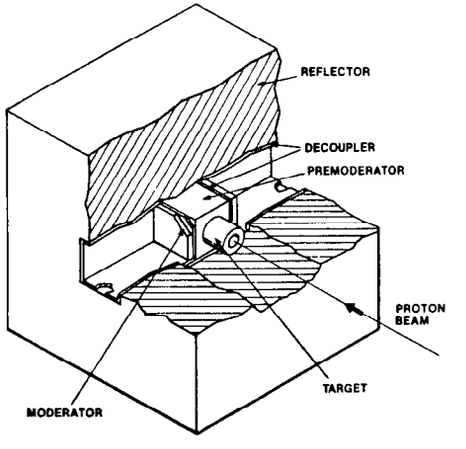

Fig. 5b This figure depicts a reflected hybrid slab-moderator; such a configuration is neutronically efficient.

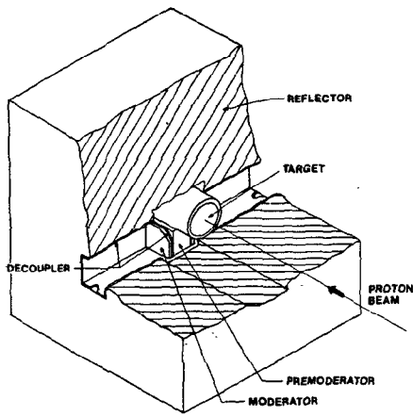

Fig. 6a This figure depicts a reflected wing-moderator. A variation of this configuration is being adopted at several pulsed spallation neutron sources around the world.

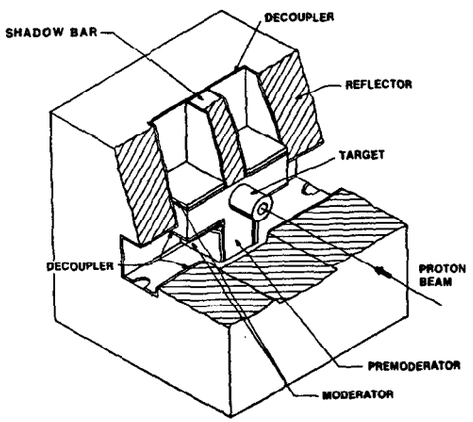

Fig. 6b This figure depicts a reflected 'T'-shape moderator. A prototype of this configuration has been installed in the WNR high-current target area.

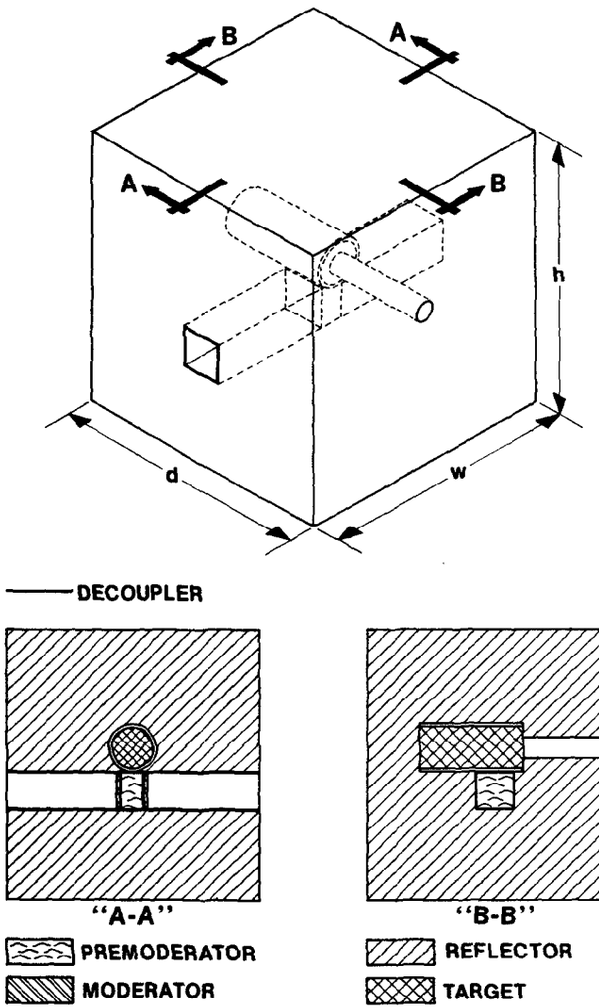

Fig. 7 Section through a reflected wing-moderator.

Fig. 9 Layout of the neutron flight paths in the WNR high-current target area.

Fig. 8a

Preliminary measured 2200 m/s neutron surface flux distribution from a reflected wing-moderator (see Fig. 6a). The distribution shown lies along the vertical center of the 9.7-cm by 9.7-cm moderator surface.

Fig. 8b

Preliminary measured 2200 m/s neutron surface flux distribution from a reflected wing-moderator (see Fig. 6a). The distribution shown lies along the horizontal center of the 9.7-cm by 9.7-cm moderator surface.

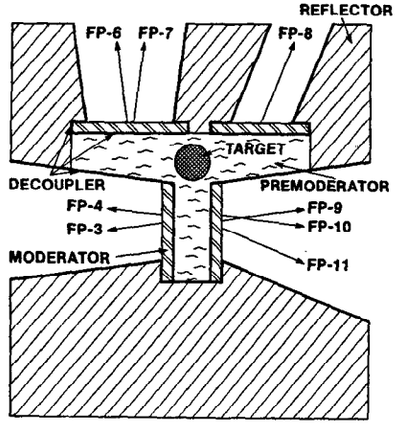

Fig. 10a Section through a reflected 'T'-shape moderator showing the location of various neutron flight paths (in the WNR high-current target area) relative to moderator surfaces.

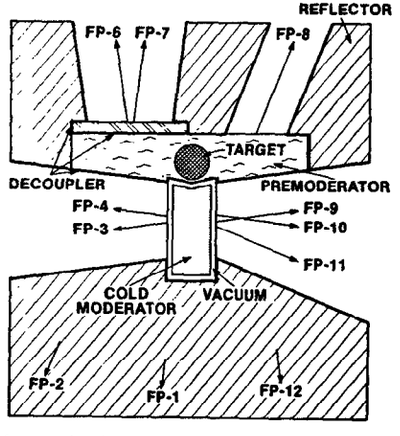

Fig. 10b Possible variation of a reflected 'T'-shape moderator which "optimizes" various moderators for each cluster of neutron flight paths.

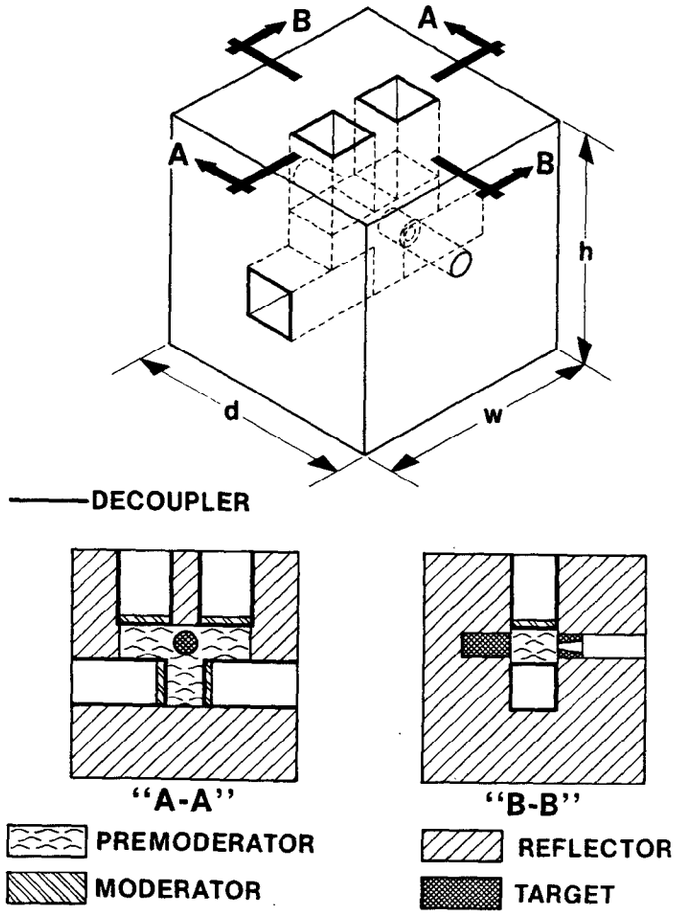

Fig. 11 Section through a reflected 'T'-shape moderator.

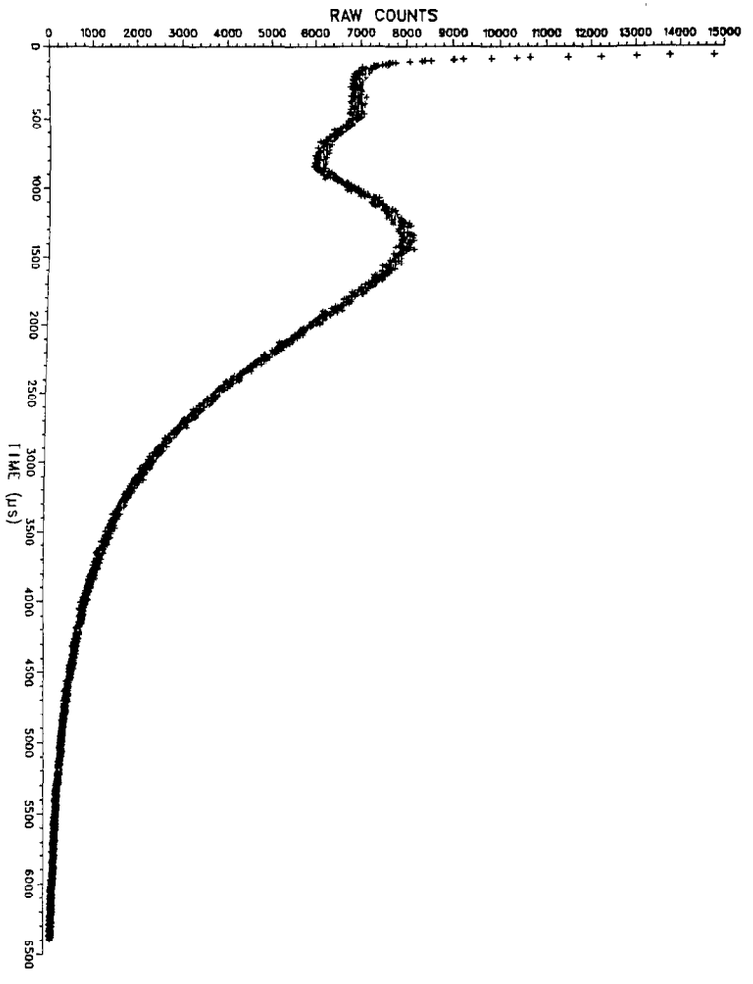

Fig. 12 Raw time-of-flight spectra obtained with a BF_3 detector.

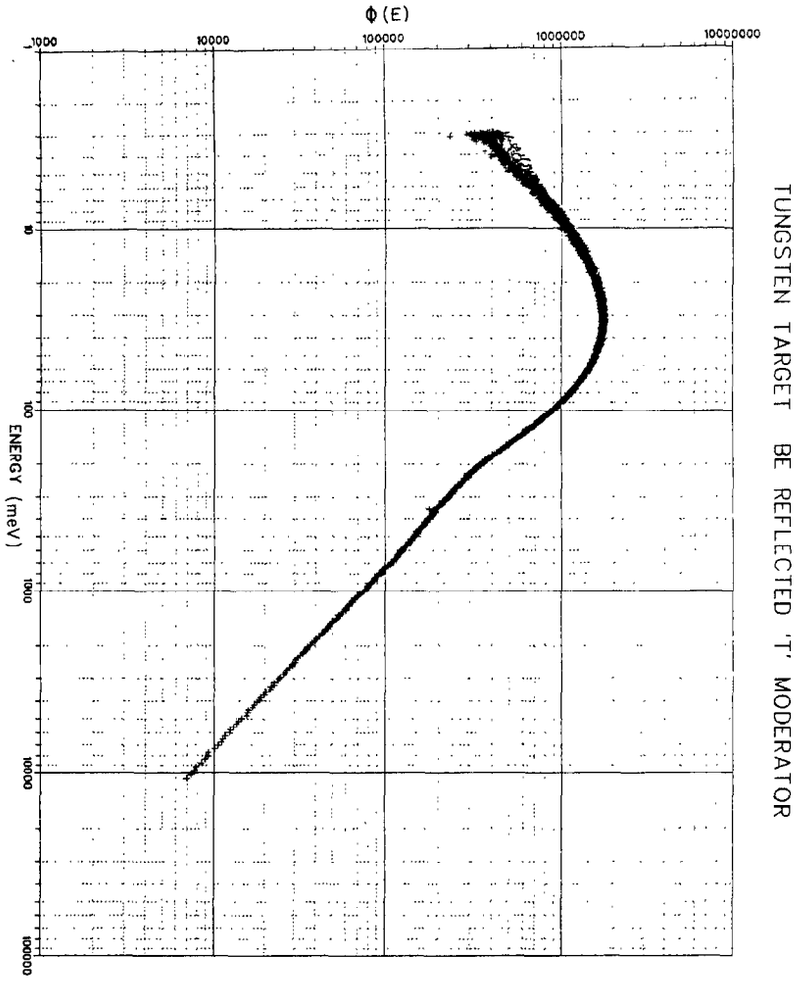

Fig. 13 Neutron spectra corrected for background and BF_3 detector efficiency.